

Seasonal variation of atmospheric total gaseous mercury and urban air quality in South India

Manikanda Bharath Karuppasamy^{1,2*}, Usha Natesan^{2*}, Karthik Ramasamy³,
Hariharan Govindasamy³, Srinivasalu Seshachalam¹

¹Institute for Ocean Management, Anna University, Chennai-600 025, Tamil Nadu, India
(<https://orcid.org/0000-0002-3159-8098>).

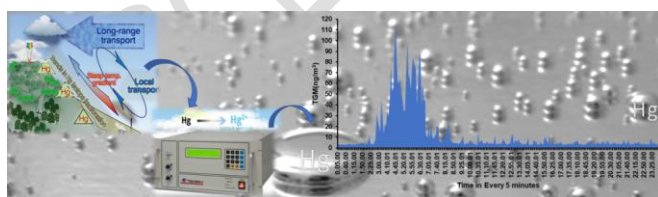
²National Institute of Technical Teachers' Training & Research (NITTTR), Chennai-600113,
Tamil Nadu, India (<https://orcid.org/0000-0003-4300-7926>).

³National Centre for Sustainable Coastal Management, Ministry of Environment, Forest and
Climate Change, Chennai Tamil Nadu, India- 600 025.

*Corresponding author

krmanibharath93@gmail.com; u_natesan@yahoo.com

GRAPHICAL ABSTRACT



Abstract

This study analyses seasonal and regular variations in ambient atmospheric concentrations of total gaseous mercury (TGM), ancillary air pollutant concentrations, and their relationship to weather conditions of a megacity environment in India. Further, to correlate with TGM concentrations at different megacities all around the urbanized environments in the world. The average concentration for TGM was $4.66 \pm 8.35 \text{ ng/m}^3$ and with an absorptions range of $0.41 \sim 540 \text{ ng/m}^3$ throughout the study period. The maximum concentration of total gaseous mercury was observed at 5.64 ng/m^3 during the winter, while the minimum concentration was 3.91 ng/m^3 during the southwest monsoon. The multivariate statistical analysis indicates the TGM values interacted positively with SR, WD, BP, CO, PM_{2.5}, NO₂, NO_x and negatively with SO₂, relative humidity, wind speed, and temperature. Meteorological parameters have an essential influence on the transport and distribution of pollutants in the monitoring site due to its location, local sources, and anthropogenic activities. Wind across India belongs to the southern hemisphere in summer and to the northern hemisphere in winter due to the movement of the intertropical convergence zone. Limited studies of atmospheric mercury concentrations have been conducted in India's city environments; however, as far as our results are concerned, they are the essentials, which exposed about environmental aggregate vaporous mercury detected in a required industrialized and coastal metropolitan zone in India.

Keywords – Ambient air quality, total gaseous mercury, ancillary air pollutants, meteorological parameter, statistical computations, global perspective.

1. Introduction

Air quality is a critical problem of growing concern to human health in urban and industrial areas of a developing country. The atmosphere contains almost a variety of pollutants emitted by various sources throughout the earth crust, including aquatic environments, marine surface, and anthropogenic emissions (Zhang et al., 2021). Atmospheric pollutants such as total gaseous mercury, particulate, and other gaseous pollutants are available at higher concentrations observed in an urban environment (Manju et al., 2018, Zhang et al., 2020; Ayyamperumal et al., 2021). Mercury naturally exists in the Earth's system. Still, decades of anthropogenic activity, including industrial, mining, and the use of fossil fuels, have mobilized growing volumes of the component in the terrestrial systems, atmospheric, coastal, and ocean region (Nguyen et al., 2021). Mercury in the atmosphere is categorized as total gaseous mercury (Hg_0), particulate mercury (Hg_p), and reactive elemental mercury (Hg^+) (Yin et al., 2020). The three most common types of mercury found in the atmosphere are gaseous mercury, elemental mercury, and particulate mercury (Xu et al., 2017; Yuan et al., 2021). The meteorological parameters play a major role in transporting and disposing air pollutants (Orioli et al., 2018; Manikanda Bharath et al., 2020). Moreover, air quality monitoring should always study meteorological parameters (Mishra, 2019). It is estimated that atmospheric pollution affects more than five million people each year globally (Aneja et al., 2001; Zhang et al., 2020). Toxic air pollution is responsible for the deaths of 1.2 million Indians, including almost 35,000 in Delhi alone (Press report: news of Indian express 2017). Air pollution has been a serious urban concern in India in recent years, and it has been related to industrial and population growth (WHO,

2014). Particularly prevalent as urban air pollution all across Indian megacities and substantial industries, thermal energy sources, and vehicles. (Kaushik et al., 2006; Schneider et al., 2021). The air pollutants affect our ecosystems, cause various diseases in human health, and drive the environment to a corrosive nature in recent years (Deb and Tsay, 2019). Pacyna et al. 2010 reported that Asian Countries are among the largest producers of global mercury emissions worldwide (Horowitz et al., 2017; Street et al., 2017). Normally Hg cycles into geochemical sources; however, the mineral reservoirs flux into the air increased in centuries through mining and the use of fossil fuels are both aspects of human activity (Amos et al., 2013; Luo et al., 2021). The average concentration of TGM in the northern region, the tropical and the southern hemisphere are (1.3–1.6 ng/m³), (1.1–1.3 ng/m³), and (0.8–1.1 ng/m³) respectively (Sprovieri et al., 2016). Various studies on TGM have been conducted across the world, focusing on urban and rural areas, as well as mining and industrial regions (Fu et al., 2016). Under the Global Mercury Observation System (GMOS) project funded by the European Commission, the atmospheric mercury content and deposition rate of mercury have been established based on long-term observations in 24 sites worldwide and additional data from 8 secondary stations (Sprovieri et al., 2016). A comprehensive study of the variation of air quality measuring up to total gaseous mercury and their connection at a high-altitude station in Southern India (Kodaikanal) had been reported (Karthik et al., 2016; Manikanda Bharath et al., 2020). While pollution by mercury is monitored in advanced countries, awareness is lacking in developing countries. However, no comprehensive study of India's established and growing metropolitan areas and their contributions to TGM has been conducted. Air quality in India's metropolises has decreased dramatically, indicating that a serious effort is required to control pollution levels for all research globally. Most urban areas in India are impacted by air pollution, which exceeds national and global limits, and mitigating measures are difficult to apply in India due to the variety of sources that impact to

local and regional environments. The study of atmospheric mercury concentration is limited in India and was carried out only in Kodaikanal in Tamil Nadu. Chennai is one of the major megacities in India with a diverse geomorphic setting, with the three major streams flowing towards the Bay of Bengal. The Cooum, Adyar, and Kosathalaiyar rivers transport the sediments derived from the hinterland. The high currents due to tidal variation redistribute the elements in the sediments, and the agitation can release the mercury trapped in the oceanic reservoir. Chennai is undergoing tremendous industrial development, and several ports, power plants, and industries are being established in the state, particularly in the coastal belt. The Bay of Bengal is one of the busy shipping corridors transporting petroleum products from the Middle East countries. The natural and industrial sources contribute significant gaseous mercury emissions, and hence, there is a need to assess the atmospheric mercury concentration and its impact on the coastal wetland ecosystem. The primary goal of this study is to characteristics and potential sources of atmospheric total gaseous mercury (TGM) in the Chennai metropolis. Further, to correlate with ancillary air pollutants associated with meteorological parameters in the study area, and also to discuss with TGM concentrations at various megacities in the world.

2. Materials and Methods

2.1. Study area

The District of Chennai lies in 13°04'2.7804" North Latitude 80°14'15.4212" Eastern longitude and is part of an Indian topography (Fig. 1). Chennai is classified as India's fourth-largest urban metropolis. The Geographical area of the Chennai district and the extent of the Chennai Metropolitan Area is 1170 sq. km. Chennai must be divided into four zones: north, central, south, and east. The northern portion is mostly an industrial sector, including

petrochemical plants in the Ambattur area near Manali, as well as other commercial industrial sectors. There are also industrial zones in Chennai's south (Guindy Industrial City) and in the western region at Sriperumbudur steel industries on the Bangalore Highway, where new start-ups of leather industries are emerging. In Manali area is most of a petrochemical plant (Chennai Petrochemical Corporation Limited, or CPCL) and other petrochemical plants situated. In Ennore region there are more than two thermal power stations are located further northern part of the study area.

The Chennai is the hub of commercials of the Indian urban city with its nearness in the Bay of Bengal has access to the business sectors in East Asia. There are three major streams area flowing as Cooum River (or Koovam) is moving through the middle, the flow of the Adyar river toward the south. These two waterways connected by the Buckingham channel, parallel to the drift. A third stream such as the Kortalaiyar river (Kosasthalayar), movements through the northern part of the city before conjunction into the Bay of Bengal. The Chennai Metropolitan is encountering dry and tropical wet climatic conditions with a normal barometrical temperature of around 25 to 40°C. The normal annual precipitation of the city is approximately 140 cm. Apart from logistics, the automobile industry, software service, health care, and manufacturing form the establishment of the financial base to the Chennai megacity.

2.2. Ambient Air Quality Measurements

The ambient air quality measurements, meteorological information and other gaseous composition of the atmosphere including particulate matter (PM_{2.5}), Total Gaseous Mercury (TGM), Sulfur Dioxide (SO₂), Carbon Monoxide (CO), Ozone (O₃), Nitric Oxide (NO), Oxides of Nitrogen (NO_x), Nitrogen Dioxide (NO₂) has been monitored in the study area. Most importantly, atmospheric total gaseous mercury was consistently observed from the

Institute for Ocean Management, Anna University, Chennai, and other pollutants were observed in pollution control board monitoring station (Fig. 1). Different gaseous information was collected from the Continuous Ambient Air Quality Monitoring Stations (CAAMS) station at the IIT, Madras, Central Pollution Control Board Chennai. Around the monitoring sites, several main roads with obvious traffic congestion, but no significant industrial source of emissions is available inside a 10 km radius. The gaseous data was observed continuous ambient air monitoring system with automatic vaporous measurement instruments, in detail, SO₂ and NO₂ were analyzed using ultraviolet fluorescence and chemiluminescence technique (CPCB) (CPCB, 2012). The Ozone (O₃) was examined by the UV photometric method and the Carbon monoxide (CO) was analyzed by non-dispersive infrared spectroscopy. For each 15-minute interval, consistent data collection of the experimental parameters was collected. Additionally, atmospheric mercury was analyzed by an ambient mercury vapour analyzer (Model No - Tekran 2537B). The Tekran 2537B is conducted to examine air "continuously" for total gaseous mercury. It analyses mercury using Cold Vapour Atomic Fluorescence Spectrophotometry (CVAFS). The instrument has been demonstrated to be linear in the range of 0.1 ng/m³ to 1500 ng/m³. The mercury vapour analyser was calibrated in automated with internal perm source every day at the time of 3.10 PM and 3.40 PM and to quantify ambient mercury concentrations, the Tekran system use CVAFS, whereas the Lumex method used Zeeman CVAAS (Karthik et al., 2016; Manikanda Bharath et al., 2020). During the intake of the ambient air sampling system, particles were removed with a 47 mm diameter Teflon filter. Hence the duration of the sample collection may be changed between every 4 minutes and every 15 minutes, and this Tekran 2537B automatically recalibrates once in every 24 hours. It runs the analysis on a regular time, according to the technique entered by the operator into the on-board computer. The Mao et al., 2008 clarifies the detail of the inspecting air and precision status of the instrument's methods. The accuracy of the

assessment and activity is 5%. To clean the instrument, zero air was used. The flow of air was collected over the PFA Teflon tube and 100 percent of RGM was a consequence of the passing competency (RGM fluctuation is sometimes 2%). The on-board computer of the instrument controls a series of valves that enter sample into one of two gold matrix cartridges at a time. The mercury in the air amalgamates onto the encased gold mesh screen when the sample goes through the cartridge. The inbuilt computer analyses the other cartridge while one cartridge samples the air. The instrument fills the cartridge with argon gas and then heating it at the start of the analysis cycle. During argon heating, mercury that has been adsorbed onto the gold matrix is emitted. The fluxes of gaseous elemental mercury concentrations in the atmosphere can also be determined directly using cavity ring spectroscopy (CRDS), a CVAAS approach that utilizes a long path optical cell. The data set acquired from this study was analysed to determine the mean and hourly variation of atmospheric mercury data and other air contaminants in relation to various meteorological factors. In this study, we are utilizing Origin 2018b, Arc GIS 10.7.1, Microsoft Excel 2016, IBM SPSS Statistics v22, Matlab vR2016b, and GeoDa software.

3. Results and Discussion

3.1. Variations of ambient total gaseous mercury and ancillary air pollutants

The gaseous mercury and other pollutants are mainly emitted from the man-made source to the atmosphere, which includes coal combustion power plants, fossil-fuel burning, incinerators for urban, fabrications of iron and steel, cement plant, chemical production facilities, medical and industrial wastes. Figure 2 shows the monthly variations of total gaseous mercury, other gaseous species, particulate matter, and meteorological parameters during the sampling periods. Table 1 and Table S1 provides the seasonal and annual variations in ambient total gaseous mercury, ancillary air pollutants and meteorological

concentration at Chennai megacity in India. Increasing the ambient concentration of these, pollutants affect the ecosystem and cause various diseases in human health (Kaushik et al., 2006). Ancillary air pollutants also harm the ecology and cause various health problems such as chlorosis and necrosis, as well as having a corrosive effect on constructed environments (Zhang et al., 2020). As illustrated in figure 2, the meteorological data set observed is performed to calculate total gaseous mercury fluctuation. Whenever the temperature (25°C) is low, the total gaseous mercury is observed to be at its highest (5.64 ng/m^3). This seems to be due to the development of haze (smoke fog) at high levels during the winter season in Chennai as compared to other seasons (CPCB, 2012). The pollution in the haze comprises dangerous vehicular and industrial pollutants, which are observed to be significantly concentrated in a metropolis like Chennai. Table 2 provides the overall statistical summary of the ambient TGM, ancillary air pollutants and meteorological concentration at Chennai megacity in India. The high concentration of the total gaseous mercury was 5.64 ng/m^3 mostly during winter, while the lowest was 3.91 ng/m^3 during the southwest monsoon. The primary contributor of ambient air mercury is in the ocean and is expected to evaporate Hg^0 from the ocean at a level of around 2900 mg/y due to anthropogenic pollution (Pirrone et al., 2010; Luo et al., 2021). Winter and summer have the largest concentrations due to long-distance transportation of total gaseous mercury comparable to autumn and spring. TGM concentrations are categorized in the following order for the four seasons: winter >summer >autumn >spring. Weather patterns and other external factors impact seasonal fluctuation. The standard deviation during southwest monsoon (spring) and winter is higher than the summer and autumn (NE Monsoon), indicating that the TGM concentrations fluctuate greatly in southwest monsoon and winter in the Chennai region. The maximum TGM content was measured in June 2016 (638.75 ng/m^3), while the lowest value was measured in August 2016 (0.1 ng/m^3). TGM concentrations in Kodaikanal, India, ranging from 1.25 ng/m^3 to 1.87

ng/m³, with a mean of 1.54 ng/m³ in 2013. The results may be impacted by the station's greater height of 2343 m, as well as emissions from the Hg thermometer factory, which had been functioning in the region since 1982 and was closed in 2001 owing to mercury toxicity problems discovered among its workers (Karthik et al., 2016). The primary sources of mercury pollution in India's mega-cities are coal-fired power plants, vehicles, industrial activity, and urban solid waste (Ayyamperumal et al., 2021). Figure 3 shows the wind rose, which describes the rising concentrations of TGM and wind speed from range of wind directions. The length of each bar represents the frequency of flow in the corresponding direction at Anna University in Chennai, India, during in the study period. TGM pollutant rose shows throughout the summer season, as increased wind speed from various wind directions. With a wind speed of 7 kmph, the rose diagram visually illustrates wind speed, and the wind direction graph shows that the SSE direction has a highest value of 9.33 percent (Fig. 3). This indicates that the accumulation of ambient gaseous mercury in the atmosphere is extreme in the SSE direction during the summer season. The Winter season pollutant rose shows that TGM vs wind speed from different wind directions displays the source of the pollutants in the monitoring station. Winter season pollutants rose shows that ENE direction has the maximum of 5.33% with a wind speed of 5 kmph (Fig. 3). This indicates that the accumulation of total gaseous mercury in the atmosphere is maximum in the ENE direction during the winter season. The southwest monsoon or spring season TGM concentration increased and wind speed from various season graphically shows wind speed and wind direction graph reveals that ENE direction has the highest value of 4.25 percent with a wind speed of 5 kmph (Fig. 3). This indicates that the accumulation of total gaseous mercury in the atmosphere is maximum in the ENE direction during the spring season. TGM pollutant rose in the autumn/fall season, as increased wind speed from various wind directions. The rose diagram visually depicts wind speed, and the wind direction graph shows that the ESE

direction has a peak value of 6.25 percent with a wind speed of 4 kmph (Fig. 3). This suggests that throughout the northeast season, the concentration of total gaseous mercury in the atmosphere is greatest in the ESE direction. From the above graphs figure 3 it is observed that when wind speed is high (14.433 kmph), the total gaseous mercury is found to be minimum (3.91 ng/m^3). This is observed during the summer season during which average wind speed is high and higher the dispersion of the air pollutants in the atmosphere and thereby reducing their concentration in the air. Temperature influences different forms of mercury. Firstly, it releases mercury from the ocean and increases the concentration of gaseous mercury. Studies have established that emission from Asian sources is about 50% of the global for the reason of anthropogenic activity (Jaffe et al., 2005; Shi et al., 2018; Yin et al., 2020). PM 2.5 was shown to be more positively correlated with total gaseous mercury and meteorological factors such as barometric pressure, temperature, wind direction, wind speed, solar radiation, and relative humidity. Coal and oil combustion may increase not just SO_2 and NO_x levels, but also TGM levels in the atmosphere. Heavy vehicles (such as diesel vehicles and boats) can also be significant contributors to SO_2 , NO_x , and Hg emissions. Though East and Southeast Asia (11.5% in terms of area) are recognized as the main contributor (~40%), South Asia (3.71%) comprising India, Pakistan and Afghanistan is third in terms of discharge and contributes about 8% of the global mercury emissions (AMAP/UNEP, 2013).

3.2. Multivariate statistical investigation

The multivariate statistical analysis was performed using GeoDa and Origin 2018b, and Microsoft Excel. The TGM, other air pollutants and meteorological parameters focus were all related to arriving at the relationship between the informational indices and were provided in Table 2. This basic statistical method was performed in Pearson's correlation matrix, scatter

plot scatter plot matrix, cluster analysis and principal component analysis. The TGM, other air pollutants and the meteorological parameters were linked to determine the relationship between the relevant indices.

3.2.1. Matrix of total gaseous mercury, ancillary air pollutants, and meteorological variables

The Pearson correlation analysis is a statistical approach for determining the strength of a variable's link by comparing it to other variables. Table 3 summarises the association between atmospheric mercury concentrations and other air contaminants with meteorological data sets. The correlation coefficient (r) was used to calculate the association between total gaseous mercury, supplementary air contaminants, and meteorological data. A significant positive correlation ($p < 0.01$) was observed in wind speed, temperature, and solar radiation (Table 3). The total gaseous mercury, meteorological parameters and ancillary air pollutants demonstrating a huge relationship (Table 3). The statistical summary was considered to be an important role a single factor matrix ($p < 0.05$) was estimated. Based on the result, the total gaseous mercury correlated positively with meteorological parameters and particulate matter including barometric pressure ($R = 0.59$), relative humidity ($R = 0.35$), solar radiation ($R = 0.34$), and $PM_{2.5}$ ($R = 0.32$); negatively with other air pollutants. Previous researches have shown that TGM concentration is likely to decrease at high O_3 and metrological concentrations, while that of RGM or Hgp is likely to increase (Selin et al., 2007, Sommar et al., 2010; Pirrone, et al., 2010). The minimum concentration of TGM has occurred in the northwestern wind direction and the maximum concentration was in the northern, northeastern wind direction. When Chennai was facing north, northeast and east winds. Also, carbon monoxide (CO) might reduce especially the higher TGM as the CO increased (Sommar et al., 2010). Specifically, coal-fired power plants have been identified as a

significant source of anthropogenic mercury emissions, as well as other pollutants released as a result of the impact of coal-fired power plants, which play a significant role in the atmospheric mercury and influence regional and local trends of discharge. This research could be helpful as standard information for TGM fixation in the urban natural condition.

3.2.2. Scatter plot and scatter plot matrix

The scatter matrix and scatter plot common tools describe the linear relationship between the variables. Every variable is arranged in such a way that it is a predictive variable and a descriptive variable. Bivariate connections between many variables including atmospheric mercury and metrological parameters visualized in the scatter matrix plot are shown in figure S1. So, each variable is loaded with different spread plots, a dependent variable, and a describing variable. The diagonal compounds cover a histogram at the variable in the corresponding column or row and its shows in figure S1 and also positive and negative and non-significant correlations. Scatter plot indicates a p value < 0.05 (*) or a p value is < 0.01 (**). Positive-negative correction is mentioned above each plot of distributed linear fit is mentioned above each plot of the distributed linear fit of the variables and distribution of each variable and strong significance shown in the histogram. We always put a predictor/independent variable as shown in figure S1. Such plots provide a simple way to see the significant properties of the structure of dependency: the disperse of points is associated with the frequency of connection, the form of the clouds will help pick an appropriate family of groups, the behaviour in the upper right-hand corner of each plot of dispersion provides qualitative details regarding tail dependency. The result showed that TGM correlated positively with meteorological parameters like barometric pressure (**), wind direction (**), solar radiation (**), relative humidity (*) and particulate matter including and also the other

air pollutants like PM_{2.5} (**) and CO (*) negatively with other air pollutants, wind speed and temperature shown in figure S1.

3.2.3. Hierarchical cluster analysis

The study of clusters was performed using the algorithmic to maximize the difference among the groups and to reduce it amid representatives of the similar group and to quantify and the quantities by the Euclidean distance (David et al., 2019). Dendrogram (ward linkage) plot was read utilizing a normal relationship linkage between the gatherings. The dendrogram is a valuable method to find grouping patterns of air quality parameters; through identified one of the variables such as TGM, other air pollutants and meteorological parameters. The meteorological information, other air pollutants and TGM fixation were connected to discover the connection between the informational collections. Dendrogram plot uncovers that the meteorological information and conveyance of TGM and other pollutants are having a similar relationship and they are fundamentally controlled by solar radiation, Figure 4 shows that the pollutant parameter is classified into three major clusters. The Clusters 1, 2 grouping is more and corresponds to cluster 3. Based on the cluster analysis the TGM was playing a major role of meteorological parameters such as solar radiation and wind speed, temperature, and relative humidity.

3.2.4. Principal Component Analysis (PCA)

Principal component analysis (PCA) is a multivariate method used to decrease the dimensionality of a collected dataset that contains a maximum number of interrelated variables, by altering them into independent variables. (Jolliffe et al., 2014; David NA et al., 2019). This method used to possible envision patterns and correlate the variables in the collected datasets and also identify the possible release sources. The extraction method based

principal component analysis, varimax with Kaiser normalization with eigenvalues of collected datasets are provided in figure 5. Cluster analysis (CA) is a valuable method to use, as a classification of tools, very convenient in pollution and ecological studies because it was simplified the variables of the PCA (David NA et al., 2019). TGM is a primary component in our studies because when more than one eigenvalue is retained (Kaiser criterion), the first component, such as TGM, is sufficient to explain 98.91 percent of the overall variance, which is dominated by the secondary component meteorological variables and can be related to wind speed and wind direction. The meteorological parameters and TGM fixation were linked to determine the relationship between the informative sets. The total variance of PCA, which is dominated by the loadings of TGM, WS, WD, Bar. Pre, Temp, RH, SR, NO₂, SO₂, and CO (loadings > 0.5) and can be associated with the source of natural source in ocean emission and man-made sources. PCA plot uncovers that the meteorological information, other air pollutants, and conveyance of TGM having a relationship, and they are fundamentally controlled by sun-oriented radiation (Fig. 5). The total rate change of the examined informational index demonstrates 98.91%. They introduce work that could be helpful as standard information for TGM fixation in the urban natural condition and anthropogenic sources. Mainly the principal components with eigenvalues of more than 1 should be an independent variable (Kaiser criterion). In our results, the total variance of the PCA with eigenvalues higher than 1 loading in total gaseous mercury, wind speed, wind direction followed by the barometric pressure. Significantly PCA loading with eigenvalues >0.5 in temperature, relative humidity, solar radiation, sulfur dioxide, nitrogen dioxide, and Carbon monoxide may be associated with the sources of industrial activity, road traffic, and fossil fuels emission shown in Fig. 5.

3.2.5. TGM concentrations and mercury emission estimated in Global

The short and long-term studies of global TGM concentrations in various megacities of the world are compared with our measurements and also, mercury emission estimated (kg) in global (Fig. S2) Table S2 provided the TGM concentration at different megacities of the world. The concentrations of TGM observed during the study period has an average distribution of 4.66 ng/m^3 , significantly higher than the Northern Hemisphere continental average levels (always 1.5 ng/m^3) (Sprovieri et al. 2016). TGM concentrations are often greater in urban and suburban areas than in rural areas (AMP 2013; Schneider et al., 2021). However, data from worldwide metropolitan locations in Asia revealed less than half of the total mean from our study. One of the primary reasons for our research area's location on the coast is that episodic dilution with cleaner ocean wind and TGM with marine bromine would decrease pollution (Zhu et al., 2012).

Mercury emission levels of 1.16 to $2.50 \text{ ng m}^{-2} \text{ h}^{-1}$ have been observed to be considerable over the oceans, but dissolved mercury concentrations at the top-water microlayer are very comparable (6.0 ng L^{-1}). The Mediterranean Sea's mean dispersion mercury ranges between 1.83 and $2.96 \text{ ng m}^{-2} \text{ h}^{-1}$, and this is the most extreme dispersion of emission (Pirrone et al., 2003; Hedgecock et al., 2006; Yuan et al., 2021). Mason (2009) has reported mercury emission from the ocean and lake basins accounting for 2778 mg/y (37 percent GEb) of ambient total gaseous mercury emission. TGM concentrations are comparable to those in East and Southeast Asia, whereas Europe, Sub-Saharan Africa, and North America have greater concentrations on overall. South Asia has the second-highest mercury emission (kg) in the world (Fig. S2), according to the AMAP/UNEP: Technical Background Study for the Global Mercury Assessment 2013. Owing to its broad health implications, local decision-makers have more worries than global problems about urban environmental challenges and would have more influence on urban environmental policies in the short term.

3.2.6. Human life and health risk of mercury

Mercury is a naturally occurring element found in atmospheric, water and soil ecosystems. It originates in the Earth's crust layer and cannot be formed or destroyed. However, natural and human activities can redistribute mercury with potentially hazardous health effects. Mercury is a powerful neurotoxin of global concern due to its chemical properties. It is a universal contaminant that travels vast distances and accumulates in the environment, thus polluting ecosystems and posing significant risks to human health. It affects as well the populations that are exposed to the source of mercury emissions, such as urban and industrial sites. In this study, human life is restricted anthropogenic activities related to mercury including food consumption of MeHg contaminated seafood. Several anthropogenic processes release mercury to the atmosphere such as mercury production process, coal, oil, and gas burning, intentional biomass burning, cement industries, Chlor-alkali industries, biomedical industries, dentistry, batteries, LED, etc. Mercury is used for various purposes. Anthropogenic activities play an important role in mercury emission, transport, and deposition. To take adequate preventing measures, it is of critical importance to upscale mercury monitoring networks and to enhance collaboration on this matter globally. This research to improve the basis of current knowledge and uncertainties in biogeochemical cycles mercury in earth systems. In future researchers to study mercury cycle from around the world to monitor the presence of mercury in ecosystems and food, chains will aid the future assessment of the effectiveness of emission reduction measures. Researchers have filled an important monitoring gap and give scientists a truly global picture of current mercury pollution levels.

4. Summary

The South Asian country going to experience unexpected growth and increasing urbanisation has a public health impact due to rising air pollution. Our results are first

reported about atmospheric total gaseous mercury in a highly industrialized urban area of South India. In our outcomes, it is displayed those other anthropogenic sources, for example, oil-based refineries and coal power plants can essentially improve the gaseous mercury centre and can also suggestively improve the atmospheric mercury level. The average concentration for TGM was $4.66 \pm 8.35 \text{ ng/m}^3$ with a range of $0.41 \sim 540 \text{ ng/m}^3$ throughout the entire study period. The relationship between TGM concentrations, wind speed and wind direction were studied. The scatter matrix, hierarchical cluster analysis (HCA) and principal component analysis (PCA) have allowed establishing the correlation between different variables. Statistical analyses indicate the significance of each parameter that allows a better analysis of possible air pollution sources and mechanisms. Furthermore, proximity to the sea a widespread natural mercury source reason for a major role of gaseous mercury in the air in the coastal region. In South Asia, some estimations of atmospheric mercury focus have been performed in the urban region, however, to the extent we know our outcomes are the essentials, which uncovered about environmental aggregate vaporous mercury seen in a necessarily industrialized urban zone in India. This research will help to suggest more efficient management approaches to monitor the environmental and human health consequences of TGM in the areas of Chennai megacity and those potentially affected by long-range transportation.

Acknowledgements

The researchers would like to express the European Commission's Global Mercury Observation System (GMOS) for providing instrumentation (Grant Agreement no. 265113) and technical assistance, as well as the National Centre for Sustainable Coastal Management (NCSCM) in Chennai for supplying meteorological data. We recognize the usage of one-year

ambient air pollutants data from the Central Pollution Control Board (IITM, Chennai) quality monitoring network in Chennai.

References

AMAP/UNEP., 2013. Technical Background Report for the Global Mercury Assessment 2013. Arctic Monitoring and Assessment Programme, Oslo, Norway/UNEP Chemicals Branch, Geneva, Switzerland. vi + 263 pp.

Amos, H.M., Jacob, D.J., Streets, D.G., and Sunderland, E.M., 2013. Legacy impacts of all-time anthropogenic emissions on the global mercury cycle. *Glob. Biogeochem. Cycles*. 27(2), 410-421. doi:10.1002/gbc.20040.

Aneja, V.P., Agarwal, A., Roelle, P.A., Phillips, S.B., Tong, Q., Watkins, N., Yablonsky, R., 2001. Measurements and analysis of criteria pollutants in New Delhi, India. *Environ. Int.* 27(1):35–42.

Ayyamperumal, R., Karuppasamy, M.B., Gopalakrishnan, G. et al. 2021. Characteristics of atmospheric total gaseous mercury concentrations (TGM) and meteorological parameters observed in Chennai metropolis, South India. *Arab. J. Geosci.* 14, 1424 <https://doi.org/10.1007/s12517-021-07803-y>

CPCB, 2012. National Ambient Air Quality Status & Trends in India—2010 (National Ambient Air Quality Monitoring NAAQMS/35/2011-2012). Online. <http://cpcb.nic.in>.

David Nuñez-Alonso., Luis Vicente Pe´rez-Arribas., Sadia Manzoor., and Jorge, O., Ca´ceres., 2019. Statistical Tools for Air Pollution Assessment: Multivariate and Spatial Analysis Studies in the Madrid Region. *J. Anal. Methods Chem.* Volume 2019, Article ID 9753927, 9 pages. <https://doi.org/10.1155/2019/9753927>.

Deb, S., Tsay, R., 2019. Spatio-Temporal Models With Space-Time Interaction And Their Applications To Air Pollution Data. *Stat. Sin.* 29(3), 1181-1207.

Hedgecock, I.M., Pirrone, N., Trunfio, G.A., and Sprovieri, F., 2006. Integrated mercury cycling, transport, and air-water exchange (MECAWEx) model. *J. Geophys. Res.* 111, D20302, doi:10.1029/2006JD007117, 2006.

Horowitz, H.M., D.J. Jacob, Y. Zhang, T.S. Dibble, F. Slemr, H.M. Amos, J.A. Schmidt, E.S. and Corbitt., 2017. A new mechanism for atmospheric mercury redox chemistry: Implications for the global mercury budget. *Atmos. Chem. Phys.* 17: 6353–6371.

Jolliffe, J., 2014. *Principal Component Analysis*, Springer-Verlag, New York, 2nd edition, 2002

Karthik, R., Paneerselvam, A., Ganguly, D., Hariharan, G., Srinivasalu, S., Purvaja, R. and Ramesh, R., 2016. Temporal variability of atmospheric Total Gaseous Mercury and its correlation with meteorological parameters at a high-altitude station of South India. *Atmos. Pollut. Res.* 8 (1), 164-173.

Kaushik, C.P., Ravindra, K., Yadav, K., Mehta, S., Haritash, A.K., 2006. Assessment of ambient air quality in urban centres of Haryana (India) in relation to different anthropogenic activities and health risks. *Environ. Monit. Assess.* 122(1-3):27-40. doi: 10.1007/s10661-005-9161-x. Epub 2006 Aug 1. PMID: 16897524.

Liu, N., Qiu, G. I., Landis, M. S., Feng, X., Fu, X., and Shang, L., 2011. Atmospheric mercury species measured in Guiyang, Guizhou province, southwest China, *Atmos. Res.* 100, 93–102.

Luo., Yuxuan Ren., Zehang Sun., Yu Li., Bing Li., Sen Yang, Wanpeng Zhang., Yuanan Hu., Hefa Cheng., 2021. Atmospheric mercury pollution caused by fluorescent lamp

manufacturing and the associated human health risk in a large industrial and commercial city, Environ. Pollut. 269, 116146, ISSN 0269-7491, <https://doi.org/10.1016/j.envpol.2020.116146>.

Manikanda Bharath, Karuppasamy., Srinivasalu, Seshachalam., Usha, Natesan., Karthik, Ramasamy., 2020. Characterization of Atmospheric Mercury in the High-Altitude Background Station and Coastal Urban City in South Asia. IntechOpen. DOI: 10.5772/intechopen.94543.

Manju, A., Kalaiselvi, K., Dhananjayan, V., Palanivel, M., Banupriya, G. S., Vidhya, M.H., Ravichandran, B., 2018. Spatio-seasonal variation in ambient air pollutants and influence of meteorological factors in Coimbatore, Southern India. Air Qual. Atmos. Health. 11(10): 1179-1189

Mason, R.P., 2009. Mercury emissions from natural processes and their importance in the global mercury cycle, Springer, New York, USA, chap. 7, 173–191.

Mishra, M., 2019. Poison in the air: Declining air quality in India. Lung India 2019; 36:160-1.

Nguyen., Guey-Rong Sheu., Xuewu Fu., Xinbin Feng., Neng-Huei Lin., 2021. Isotopic composition of total gaseous mercury at a high-altitude tropical forest site influenced by air masses from the East Asia continent and the Pacific Ocean, Atmos. Environ. Volume 246, 118110, ISSN 1352-2310, <https://doi.org/10.1016/j.atmosenv.2020.118110>.

Orioli, R., Cremona, G., Ciancarella, L., Solimini, A.G., 2018. Association between PM 10, PM2. 5, NO2, O3 and self-reported diabetes in Italy: A cross-sectional, ecological study. PLoS One. 13(1): 0191112.

Pacyna, E.G., Pacyna, J.M., Sundseth, K., Munthe, J., Kindbom, K., Wilson, S., Steenhuisen, F. and Maxson, P., 2010. Global emission of mercury to the atmosphere from anthropogenic sources in 2005 and projections to 2020. *Atmos. Environ.* 44, 2487-2499.

Pirrone, N., Cinnirella, S., Feng, X., Friedli, H. R., Levine, L., Pacyna, J., Pacyna, E. G., Streets, D. G., and Sundseth, K., 2010. HTAP 2010 Assessment Report – Emissions and Projections, Tech. Rep. Chapter B3, LRTAP – Task Force on Hemispheric Transport of Air Pollutants, <http://htap.icg.fz-juelich.de/data/ChapterB3>, 2010.

Pirrone, N., Stracher, G.B., Cinnirella, S., Feng, X., Finkelman, R.B., Friedli, H.R., Leaner, J., Mason, R., Mukherjee, A.B., Streets, D.G., Telmer, K., 2010. Global mercury emissions to the atmosphere from anthropogenic and natural sources. *Atmos. Chem. Phys.* 10, 5951–5964.

Press report: <http://www.newindianexpress.com/nation/2017/jan/11/pollution-killing-1.2-million-people-annually-in-india-1558610.html>.

Press report: <https://www.blogs.timesofindia.indiatimes.com/jugglebandhi/dilli-chodo-thanks-to-its-deadly-pollution-people-are-fleeing-the-capital-or-are-they-f0-9f-98-9c/>.

Rutter, A.P., Snyder, D.C., Stone, E.A., Schauer, J.J., Gonzalez-Abraham, R., Molina, L.T., Márquez, C., Cárdenas, B., and de Foy, B. 2009. In situ measurements of speciated atmospheric mercury and the identification of source regions in the Mexico City Metropolitan Area, *Atmos. Chem. Phys.* 9, 207–220, doi:10.5194/acp-9-207-2009.

Schneider, Neil L. Rose., Lauri Myllyvirta., Simon Haberle., Anna Lintern., Jingjing Yuan., Darren Sinclair., Cameron Holley., Atun Zawadzki., Ruoyu Sun., 2021. Mercury atmospheric emission, deposition and isotopic fingerprinting from major coal-fired power plants in Australia: Insights from palaeo-environmental analysis from sediment cores. *Environ. Pollut.* 287, 117596, ISSN 0269-7491, <https://doi.org/10.1016/j.envpol.2021.117596>.

Selin, N.E., Jacob, D.J., Park, R.J., Yantosca, R.M., Strode, S., Jaeglé, L. and Jaffe, D., 2007. Chemical Cycling and Deposition of Atmospheric Mercury: Global Constraints from Observations. *J. Geophys. Res.* 112: 1–14.

Shi, Y., Matsunaga, T., Yamaguchi, Y., Li, Z., Gu, X., Che, X., 2018. Long-term trends and spatial patterns of satellite-retrieved PM_{2.5} concentrations in South and Southeast Asia from 1999 to 2014, *Sci. Total. Environ.*, 615 pp. 177–186

Slemr, F., Martin, L., Labuschagne, C., Mkololo, T., Angot, H., Magand, O., Dommergue, A., Garat, P., Ramonet, M., and Bieser, J., 2020. Atmospheric mercury in the Southern Hemisphere – Part 1: Trend and inter-annual variations in atmospheric mercury at Cape Point, South Africa, in 2007–2017, and on Amsterdam Island in 2012–2017, *Atmos. Chem. Phys.* 20, 7683–7692, <https://doi.org/10.5194/acp-20-7683-2020>, 2020.

Sommar, J., Andersson, M.E. and Jacobi, H.W., 2010. Circumpolar Measurements of Speciated Mercury, Ozone and Carbon Monoxide in the Boundary Layer of the Arctic Ocean. *Atmos. Chem. Phys.* 10: 5031–5045.

Sonke, J.E., 2016. Atmospheric mercury speciation dynamics at the high-altitude Pic du Midi Observatory, Southern France. *Atmos. Chem. Phys.* 16, 5623–5639.

Sprovieri, F., Pirrone, N., Bencardino, M., D'Amore, F., Carbone, S., Cinnirella, F., Mannarino, V. and Landis, M., 2016. Atmospheric mercury concentrations observed at ground-based monitoring sites globally distributed in the framework of the GMOS network. *Atmos. Chem. Phys.* 16: 11915–11935.

Streets, D.G., Horowitz, H.M., Jacob, D.J., Lu, Z., Levin, L., TerSchure, A.F.H., and Sunderland, E.M., 2017. Total mercury released to the environment by human activities. *Environ. Sci. Technol.* 51: 5969–5977.

Wang, X.C., Feng, H., Ma, H.Q., 2007. 2/21553.11822/21553" contamination in surface sediments of Jiaozhou Bay, Qingdao, Clean - Soil Air Water. vol. 35, pp. 62-70.

WHO, 2014. WHO Air Quality Guidelines. <http://www.who.int/mediacentre/news/releases/2014/air-pollution/en/>.

Xu, X., Liao, Y., Cheng, I., and Zhang, L., 2017. Potential sources and processes affecting speciated atmospheric mercury at Kejimikujik National Park, Canada: comparison of receptor models and data treatment methods, Atmos. chem. Phys. 17, 1381–1400 <https://doi.org/10.5194/acp-171381-2017>.

Yin, X., Zhou, W., Kang, S., de Foy, B., Yu, Y., Xie, J., Sun, S., Wu, K., Zhang, Q., 2020. Latest observations of total gaseous mercury in a megacity (Lanzhou) in northwest China Sci. Total. Environ., 720 p. 137494, 10.1016/j.scitotenv.2020.137494

Yuan., Ruoyu Sun., Ruwei Wang., Biao Fu., Mei Meng., Wang Zheng., Jiubin Chen., 2021. Denitrification devices in urban boilers change mercury isotope fractionation signatures of coal combustion products, Environ. Pollut. 268, Part B, 115753, ISSN 0269-7491, <https://doi.org/10.1016/j.envpol.2020.115753>.

Zhang, L., An, J., Liu, M., Li, Z., Liu, Y., Tao, L., Liu, X., Zhang, F., Zheng, D., Gao, Q., Guo, X., Luo, Y., 2020. Spatiotemporal variations and influencing factors of PM^{2.5} concentrations in Beijing, China, Environ. Pollut. doi: <https://doi.org/10.1016/j.envpol.2020.114276>.

Zhang, Y., Song, Z., Huang, S. et al., 2021. Global health effects of future atmospheric mercury emissions. Nat. Commun. 12, 3035. <https://doi.org/10.1038/s41467-021-23391-7>

Zhu, J., Wang, T., Talbot, R., Mao, H., Hall, C. B., Yang, X., Fu, C., Zhuang, B., Li, S., Han, Y., and Huang, X., 2012. Characteristics of atmospheric Total Gaseous Mercury (TGM)

observed in urban Nanjing, China, Atmos. Chem. Phys., 12, 12103–12118,
<https://doi.org/10.5194/acp-12-12103-2012>, 2012.

ACCEPTED MANUSCRIPT

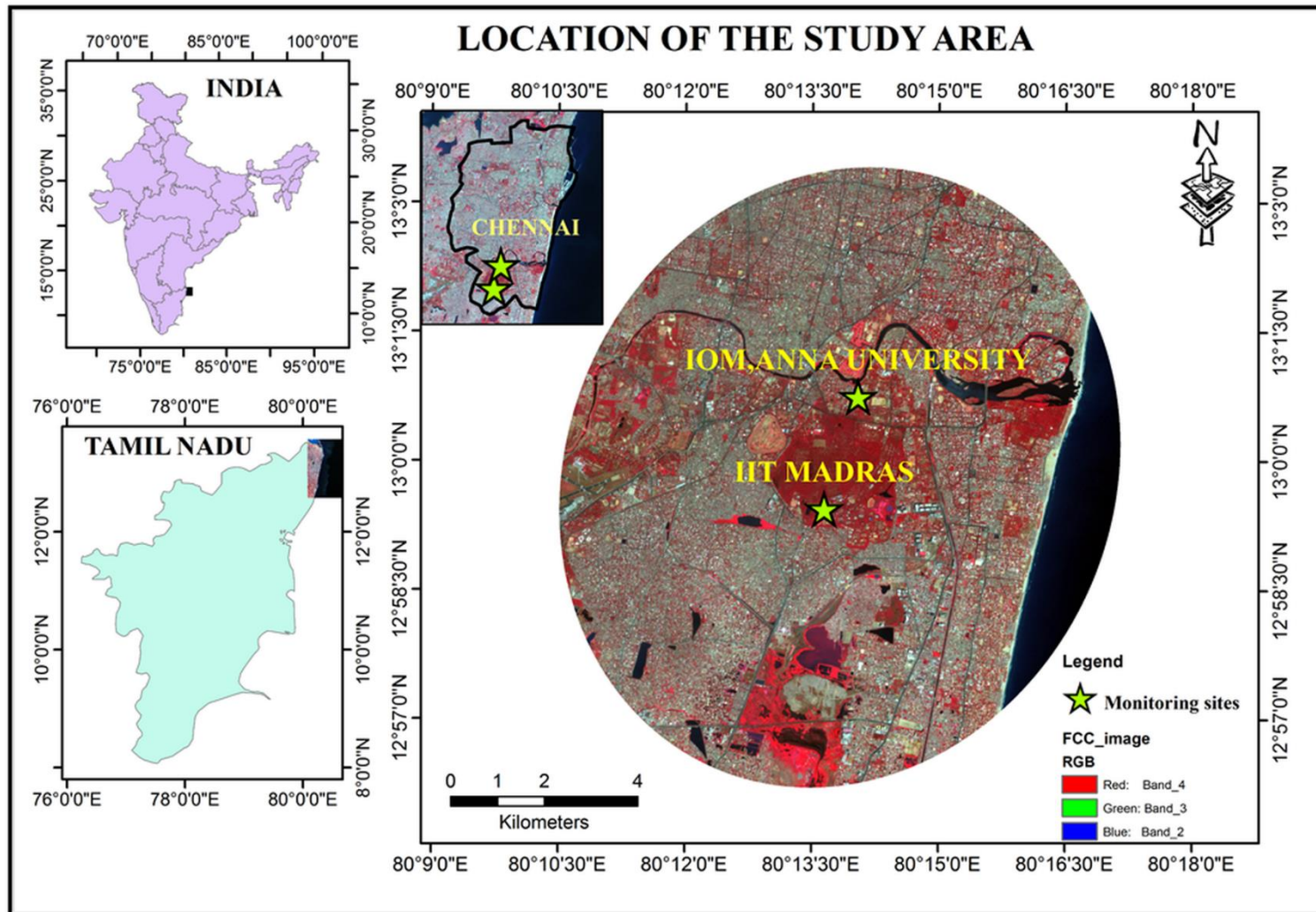


Fig. 1. A map showing location of the study area and ambient air quality monitoring sites

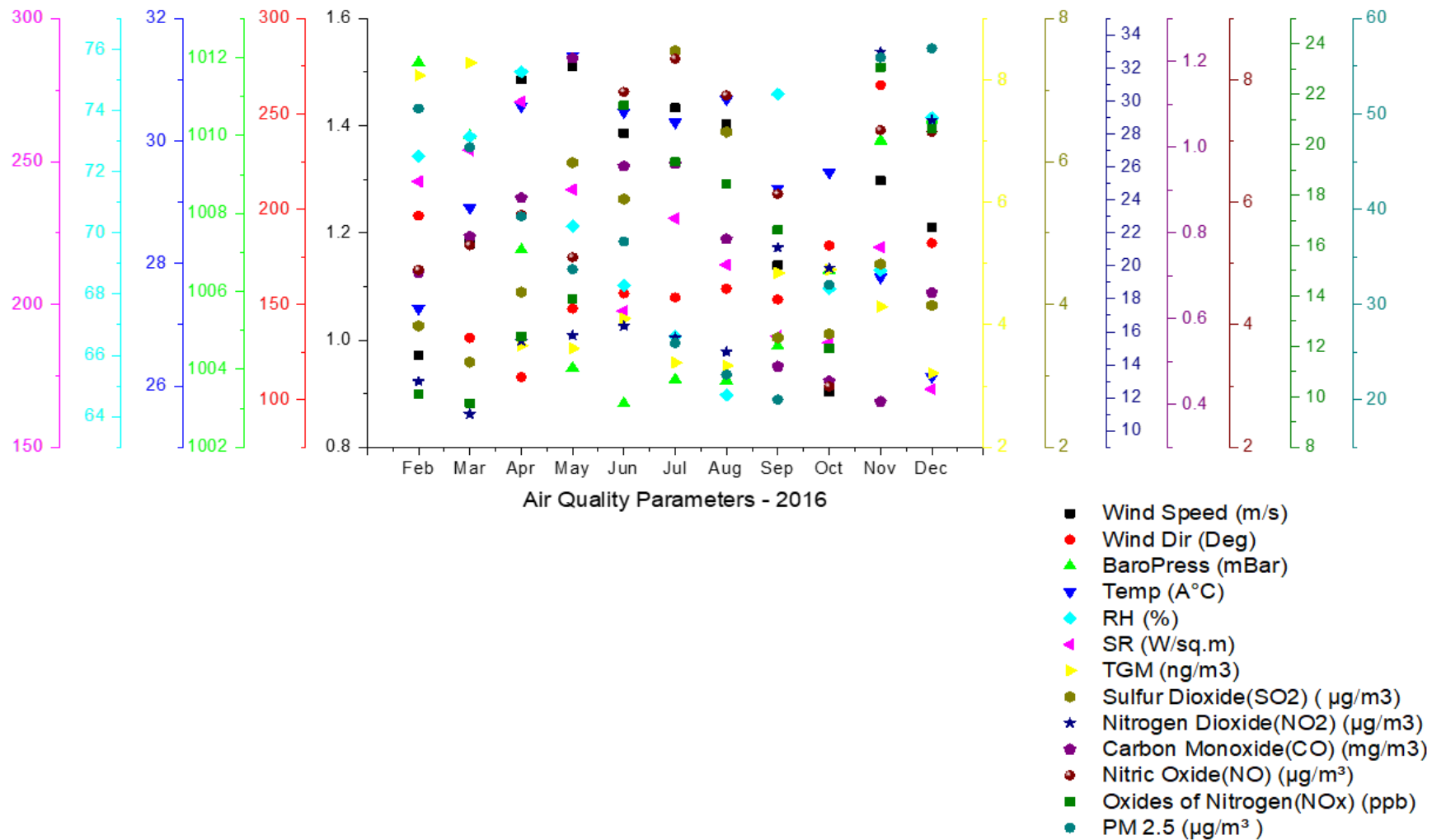


Fig. 2. Average monthly variations of total gaseous mercury, other gaseous species, particulate matter and meteorological parameters during the sampling period

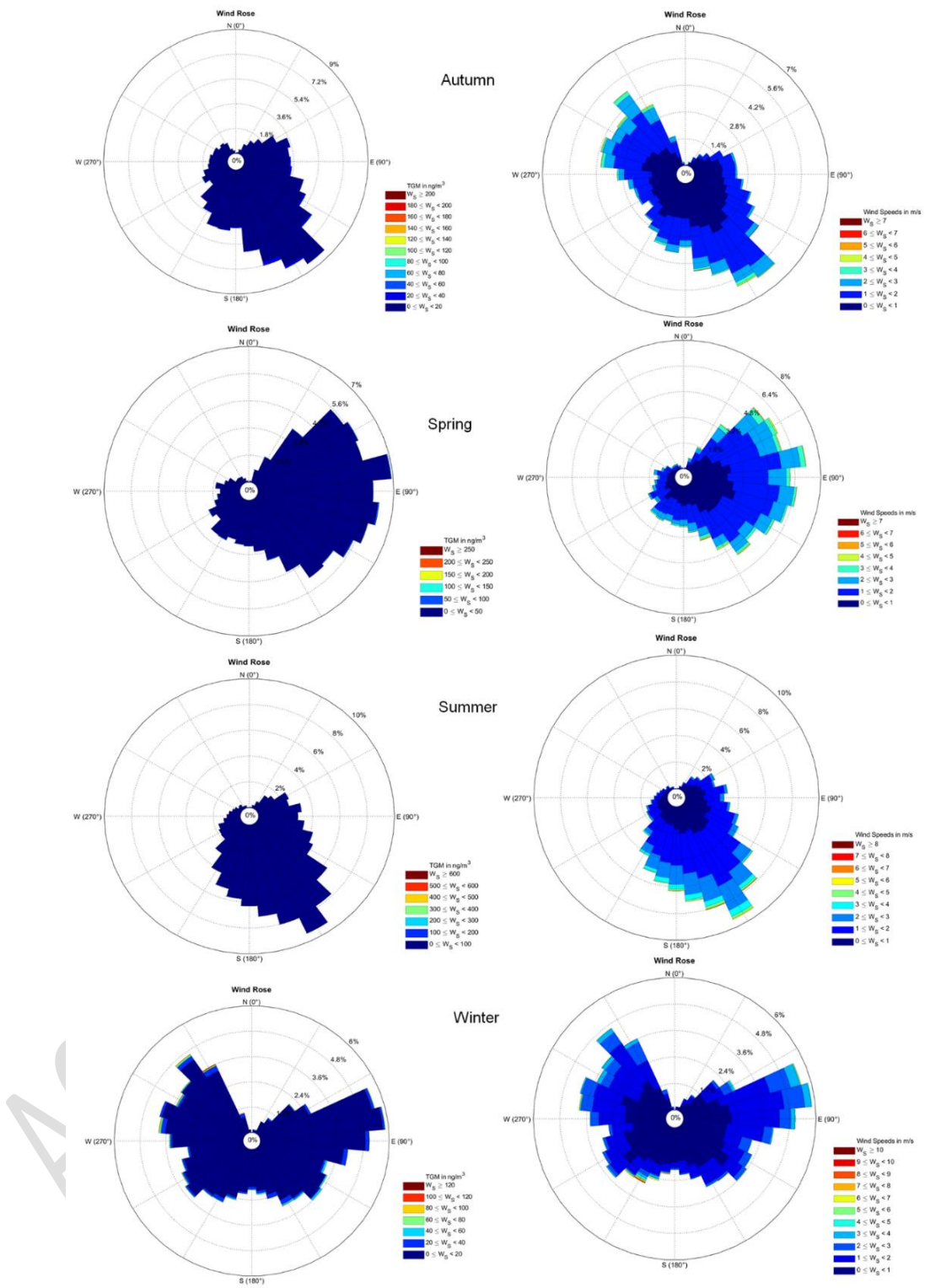


Fig. 3. Concentration rose of TGM and Wind speed from different wind directions. The length of each spoke describes the frequency of flow from the corresponding direction during the sampling period at Anna University, Chennai, India

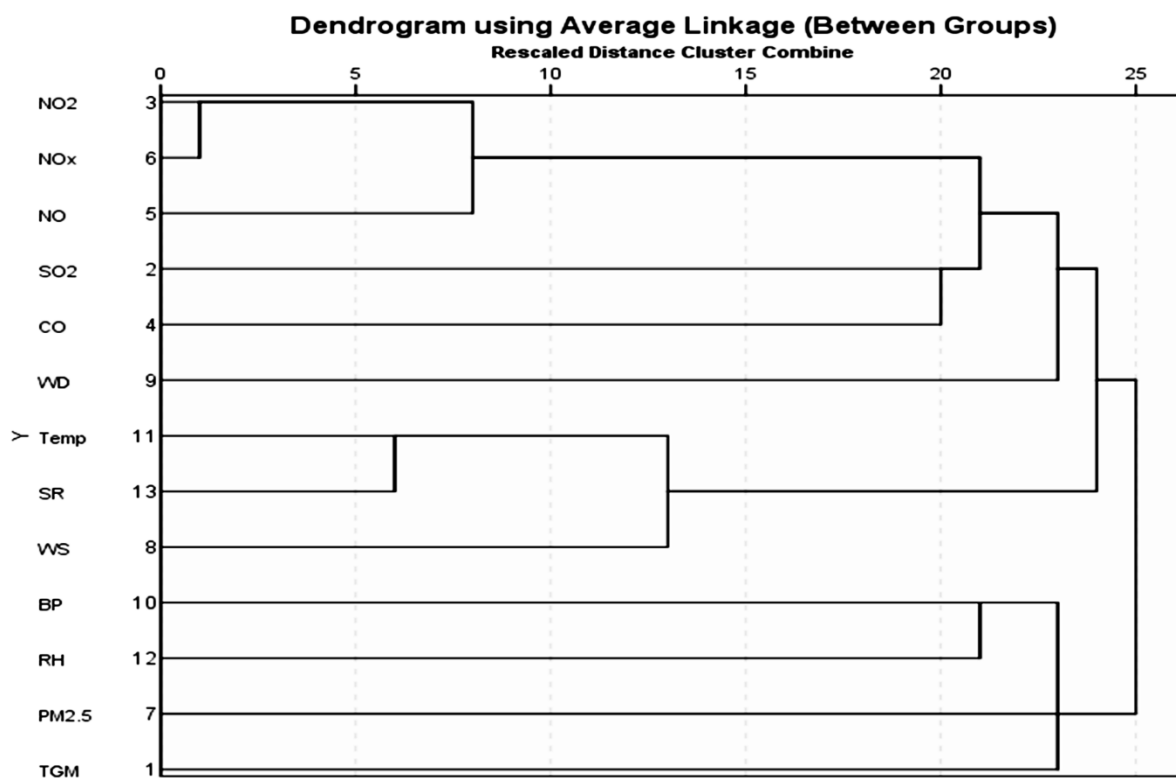
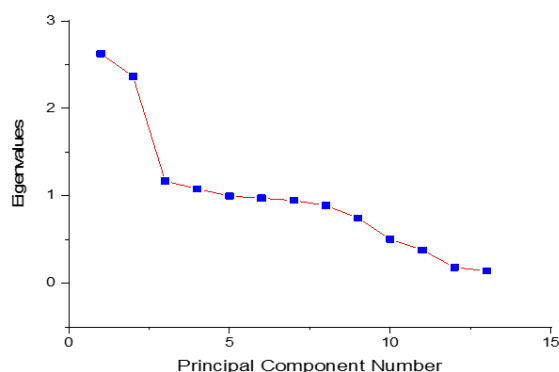


Fig. 4. Dendrogram of the total gaseous mercury, meteorological parameters, and ancillary air pollutants concentration

Extraction Method: Principal Component Analysis.
Rotation Method: Varimax with Kaiser Normalization.



Variables	PCA	Eigenvalues	PCA
TGM	1	2.62	
Wind Speed (m/s)	2	2.37	20.19%
Wind Dir (Deg)	3	1.17	18.19%
BaroPress (mBar)	4	1.08	8.99%
Temp (°C)	5	0.99	8.31%
RH (%)	6	0.97	7.68%
SR (W/sq.m)	7	0.95	7.49%
Sulfur Dioxide(SO ₂)- (µg/m ³)	8	0.88	7.29%
Nitrogen Dioxide(NO ₂)- (µg/m ³)	9	0.75	6.84%
Carbon Monoxide (CO)-(mg/m ³)	10	0.50	5.73%
Nitric Oxide(NO)- (µg/m ³)	11	0.37	3.88%
Oxides of Nitrogen(NO _x)-(ppb)	12	0.18	2.92%
PM 2.5-(µg/m ³)	13	0.14	1.40%

Fig. 5. The principal components analysis of all air quality parameters, each point represents an air pollutant of the variables

Table 1. Seasonal variation of total gaseous mercury and other air quality parameters measured in Chennai megacity

Air Quality Parameters	Average			
	Autumn	Spring	Summer	Winter
Sulfur Dioxide (SO ₂) (µg/m ³)	3.87	4.45	6.54	3.81
Nitrogen Dioxide (NO ₂) (µg/m ³)	24.33	14.05	15.44	18.87
Carbon Monoxide (CO) (mg/m ³)	0.45	0.96	0.88	0.69
Nitric Oxide (NO) (µg/m ³)	5.36	5.42	7.95	5.72
Oxides of Nitrogen (NO _x) (ppb)	16.97	12.00	19.49	14.01
Particulate Matter (PM 2.5) (µg/m ³)	35.21	39.53	26.93	52.85
Wind Speed (m/s)	1.13	1.38	1.41	1.11
Wind Direction (Deg)	198.18	131.09	156.58	187.29
Barometric Pressure (mBar)	1006.88	1006.86	1003.43	1010.55
Temperature (°C)	28.80	30.31	30.50	26.56
Relative Humidity (RH) (%)	71.00	72.81	66.54	73.26
Solar Radiation (SR) (W/sq.m)	199.49	254.52	212.50	197.78
Total Gaseous Mercury (TGM) (ng/m ³)	4.69	5.40	3.62	5.39

Table 2. Statistical summary of the ambient total gaseous mercury, ancillary air pollutants and meteorological concentration at Chennai megacity

Statistical summary														
Parameters	TGM	SO ₂	NO ₂	CO	NO	NO _x	PM _{2.5}	WS	WD	BP	Temp	RH	SR	
N	Valid	21682	21792	21774	21829	21822	21774	21833	24089	24089	24089	24089	24089	24089
	Missing	4380	4270	4288	4233	4240	4288	4229	1973	1973	1973	1973	1973	1973
Mean	4.66	4.48	17.84	.75	5.87	14.97	37.72	1.29	161.68	1006.23	29.50	70.46	221.04	
Std. Error of Mean	.057	.054	.096	.01	.046	.079	.63	.01	.49	.08	.02	.09	1.97	
Median	2.97 ^a	3.56 ^a	13.45 ^a	.65 ^a	3.85 ^a	12.23 ^a	28.98 ^a	1.15 ^a	150.82 ^a	1005.87 ^a	29.37 ^a	71.87 ^a	7.41 ^a	
Mode	2.47	0.00	0.00	.28	0.00	0.00	0.00	.91	138.29 ^c	1004.34	25.97	87.81 ^c	0.00	
Std. Deviation	8.35	7.92	14.13	.68	6.86	11.72	93.61	.79	77.07	12.43	2.95	14.38	305.11	
Variance	69.79	62.65	199.86	.47	47.19	137.42	8763.15	.62	5940.65	154.65	8.73	206.99	93089.21	
Range	539.64	999.99	246.80	42.70	119.34	388.44	5994.58	9.69	347.86	872.22	37.09	88.87	1191.97	
Minimum	.41	0.00	0.00	0.00	0.00	0.00	0.00	.03	5.00	143.39	3.49	11.30	0.00	
Maximum	540.05	999.99	246.80	42.70	119.34	388.44	5994.58	9.73	352.86	1015.61	40.58	100.18	1191.97	
Percentiles	25	2.31 ^b	2.17 ^b	7.93 ^b	.39 ^b	2.05 ^b	6.68 ^b	15.98 ^b	.72 ^b	102.05 ^b	1003.59 ^b	27.53 ^b	60.04 ^b	.01 ^b
Percentiles	50	2.97	3.56	13.45	.68	3.85	12.23	28.99	1.15	150.83	1005.87	29.37	71.87	7.42
Percentiles	75	4.46	5.82	24.12	.97	6.70	19.91	48.31	1.71	210.81	1009.37	31.29	81.27	414.08

a. Calculated from grouped data.

b. Percentiles are calculated from grouped data.

c. Multiple modes exist. The smallest value is shown

Sulfur Dioxide, (SO₂) (µg/m³); Nitrogen Dioxide (NO₂) (µg/m³); Carbon Monoxide (CO) (mg/m³); Nitric Oxide

(NO) ($\mu\text{g}/\text{m}^3$); Oxides of Nitrogen (NO_x) (ppb); Particulate Matter (PM 2.5) ($\mu\text{g}/\text{m}^3$) Wind Speed (WS) (m/s); Wind Direction (Deg); Barometric Pressure (mBar); Temperature ($\hat{\text{A}}^\circ\text{C}$); Relative Humidity (RH) (%); Solar Radiation (SR) (W/sq.m); Total Gaseous Mercury (TGM) (ng/m^3).

Table 3. Correlation matrix of total gaseous mercury, ancillary air pollutants and meteorological variables at Chennai megacity

Correlation matrix	Wind Speed (m/s)	Wind Dir (Deg)	Baro Press (mBar)	Temp ($\hat{\text{A}}^\circ\text{C}$)	RH (%)	SR (W/sq.m)	TGM (ng/m^3)	Sulfur Dioxide (SO_2) ($\mu\text{g}/\text{m}^3$)	Nitrogen Dioxide (NO_2) ($\mu\text{g}/\text{m}^3$)	Carbon Monoxide (CO) (mg/m^3)	Nitric Oxide (NO) ($\mu\text{g}/\text{m}^3$)	Oxides of Nitrogen (NO _x) (ppb)	PM 2.5 ($\mu\text{g}/\text{m}^3$)
Wind Speed (m/s)	1												
Wind Dir (Deg)	-0.35	1											
BaroPress (mBar)	-0.54	0.44	1										
Temp ($\hat{\text{A}}^\circ\text{C}$)	0.59	-0.59	-0.85	1									
RH (%)	-0.21	-0.26	0.50	-0.39	1								
SR (W/sq.m)	0.37	-0.34	0.15	0.34	0.19	1							
TGM (ng/m^3)	-0.62	0.04	0.59	-0.35	0.35	0.34	1						
Sulfur Dioxide (SO_2) ($\mu\text{g}/\text{m}^3$)	0.7	-0.10	-0.67	0.57	-0.72	0.08	-0.60	1					
Nitrogen Dioxide (NO_2) ($\mu\text{g}/\text{m}^3$)	-0.09	0.73	0.27	-0.55	0.04	-0.56	-0.40	-0.16	1				
Carbon Monoxide (CO) (mg/m^3)	0.70	-0.61	-0.45	0.61	-0.12	0.47	-0.20	0.59	-0.59	1			
Nitric Oxide (NO) ($\mu\text{g}/\text{m}^3$)	0.62	0.07	-0.32	0.05	-0.34	-0.13	-0.49	0.63	0.21	0.22	1		
Oxides of Nitrogen (NO _x) (ppb)	0.39	0.45	-0.29	-0.09	-0.42	-0.53	-0.67	0.47	0.66	-0.11	0.80	1	
PM 2.5 ($\mu\text{g}/\text{m}^3$)	-0.21	0.51	0.86	-0.75	0.36629	0.09	0.32	-0.45	0.42	-0.21	-0.08	0.03	1

Seasonal variation of atmospheric total gaseous mercury and urban air quality in South India

**Manikanda Bharath Karuppasamy^{1,2*}, Usha Natesan^{2*}, Karthik Ramasamy³,
Hariharan Govindasamy³, Srinivasalu Seshachalam¹**

¹Institute for Ocean Management, Anna University, Chennai-600 025, Tamil Nadu, India
(<https://orcid.org/0000-0002-3159-8098>).

²National Institute of Technical Teachers' Training & Research (NITTTR), Chennai-600113,
Tamil Nadu, India (<https://orcid.org/0000-0003-4300-7926>).

³National Centre for Sustainable Coastal Management, Ministry of Environment, Forest and
Climate Change, Chennai Tamil Nadu, India- 600 025.

*Corresponding author

krmanibharath93@gmail.com; u_natesan@yahoo.com

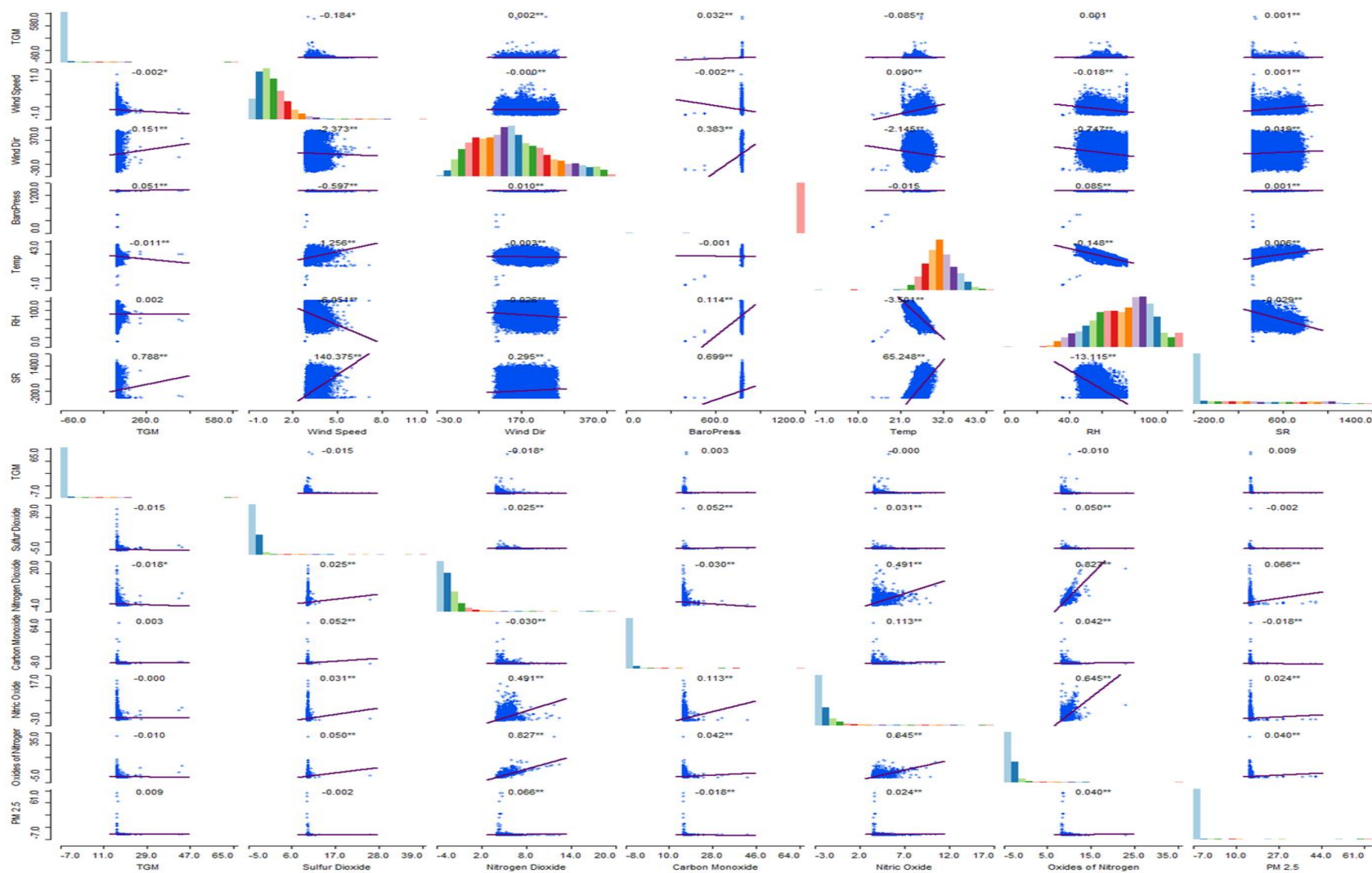
Table S1. The seasonal and annual variations in ambient total gaseous mercury, ancillary air pollutants and meteorological concentration at Chennai megacity in India

Air Quality Parameters	Autumn				Spring				Summer				Winter			
	Minimum	Maximum	Average	Standard deviation	Minimum	Maximum	Average	Standard deviation	Minimum	Maximum	Average	Standard deviation	Minimum	Maximum	Average	Standard deviation
Sulfur Dioxide (SO₂) (µg/m³)	0.02	999.99	3.87	13.50	0.02	121.49	4.45	3.23	0.02	137.38	6.54	4.80	0.02	50.93	3.81	3.12
Nitrogen Dioxide (NO₂) (µg/m³)	0.10	218.99	24.33	16.07	0.03	246.80	14.05	11.32	0.98	224.51	15.44	11.59	0.31	140.36	18.87	15.04
Carbon Monoxide (CO) (mg/m³)	0.01	10.00	0.45	0.38	0.01	25.71	0.96	0.58	0.01	10.00	0.88	0.60	0.01	42.70	0.69	1.14
Nitric Oxide (NO) (µg/m³)	0.04	119.34	5.36	6.55	0.01	101.86	5.42	5.19	0.02	72.56	7.95	8.21	0.04	110.50	5.72	8.91
Oxides of Nitrogen	0.05	149.34	16.97	11.98	0.02	126.36	12.00	9.04	1.30	388.44	19.49	13.53	1.16	111.41	14.01	12.64

(NO _x)- (ppb)																
PM 2.5 (µg/m ³)	0.03	456.01	35.21	30.40	0.45	5994.5 8	39.53	145.02	0.19	292.67	26.93	22.58	0.03	247.04	52.85	27.84
Wind Speed (m/s)	0.05	6.76	1.13	0.70	0.06	6.23	1.38	0.78	0.06	7.18	1.41	0.80	0.04	9.73	1.11	0.84
Wind Dir (Deg)	6.86	352.86	198.1 8	82.89	5.00	352.86	131.0 9	69.36	10.86	345.57	156.5 8	57.10	6.14	348.29	187.2 9	91.14
BaroPress (mBar)	998.66	1013.9 2	1006. 88	2.96	144.17	1014.4 0	1006. 86	15.46	430.86	1008.4 4	1003. 43	13.22	144.54	1015.6 1	1010. 55	17.79
Temp (Â°C)	23.20	37.08	28.80	2.49	4.03	40.58	30.31	2.70	12.29	38.63	30.50	2.74	3.49	32.41	26.56	2.36
RH (%)	27.63	100.18	71.00	14.99	11.48	100.17	72.81	12.37	32.31	100.17	66.54	14.98	11.30	100.18	73.26	14.44
SR (W/sq.m)	0.00	1128.2 0	199.4 9	281.28	0.00	1191.9 7	254.5 2	337.61	0.00	1102.4 5	212.5 0	292.56	0.00	992.10	197.7 8	283.34
TGM (ng/m ³)	0.84	196.76	4.69	5.68	0.82	203.98	5.40	7.72	0.73	540.05	3.62	9.45	0.41	110.59	5.39	8.69

Table S2. The TGM concentration at different megacities of the world

Locations	Types	Duration	TGM (ng/m³)	Reference
Fort McMurray, Alberta, Canada	Urban	2½ years	1.45 ± 0.18	Matthew et al., (2013)
Reno, USA	Urban	3 years	1.6	Peterson et al., (2009)
Tokai-mura, Japan	Urban	11 months	3.78 ± 1.62	Osawa et al., (2007)
Detroit, Michigan, USA	Urban	1 year	2.5 ± 1.4	Liu et al., (2010)
Seoul, Korea	Urban	5 year	5.06	Kim et al., (2015)
Beijing	Urban	60 days	4.9 - 8.3	Wang et al., (2007)
Changchun, Jilin	Urban	1 year	13.5 - 25.4	Feng et al., (2004)
Guangzhou, Guangdong	Urban	2 weeks	13.5 ± 7.1	Wang et al., (2009)
Mexico city, Mexico	Urban	17 days	7.2 ± 4.8	Rutter et al., (2009)
Nanjing, Jiangsu	Urban	1 year	7.94 ± 6.99	Zhu J et al., 2012
Ningbo, Zhejiang	Urban	12 days	3.79 ± 1.29	Nguyen et al., (2009)
Guiyang, Guizhou	Urban	1 year	8.40 ± 4.87	Feng et al., (2004)
Guiyang, Guizhou	Urban	6 months	7.4 ± 4.8, 6.2 ± 5.1	Liu et al., (2011)
Chennai	Urban	1 year	4.6	Present Study



1
 2 **Fig. S1.** Scatter matrix plot with smoothing of the TGM versus meteorological parameters and TGM versus other air pollutant variables,
 3 histograms of the variables in the diagonal, and correlation coefficients in the upper part of the matrix and highlight the dependence patterns.

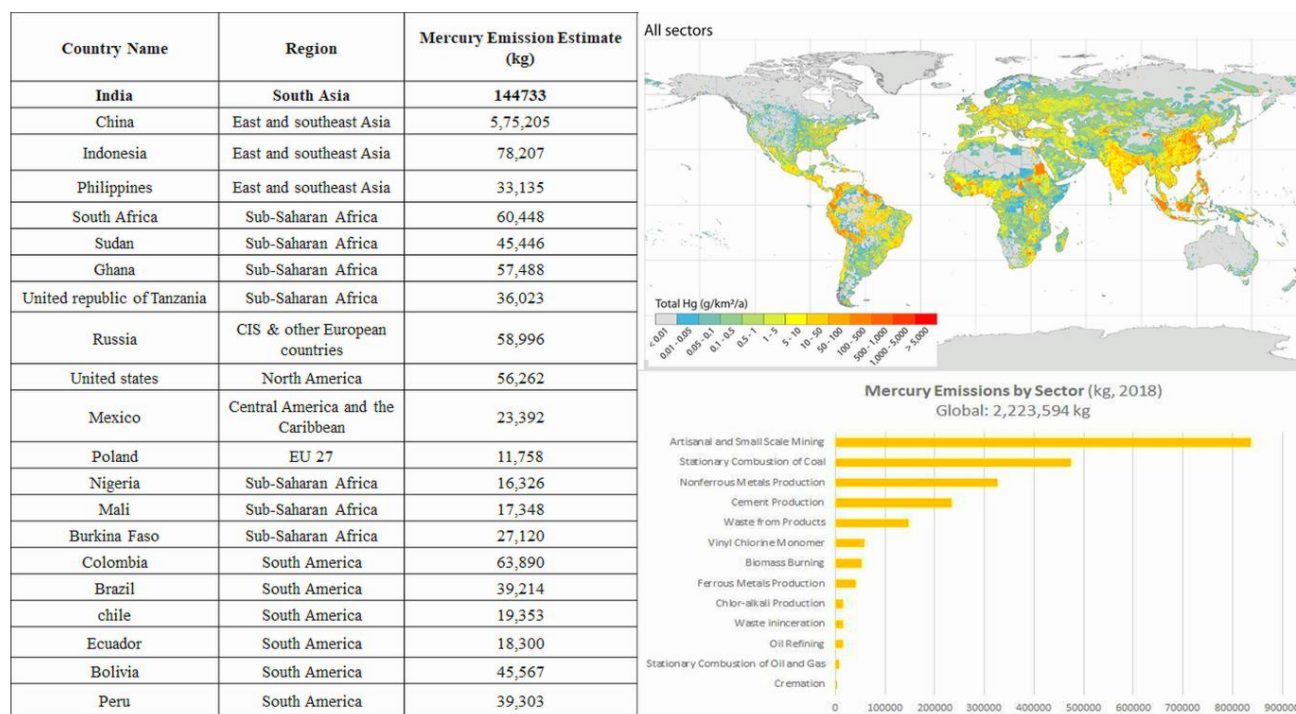


Fig. S2. Mercury emission estimated (kg) in India and other countries.

4
5
6
7
8
9
10